Low-bias gate tunable terahertz plasmonic signatures in chemical vapour deposited graphene of varying grain size

Citation: Kamboj, Varun S., et al. "Low-Bias Gate Tunable Terahertz Plasmonic Signatures in Chemical Vapour Deposited Graphene of Varying Grain Size." Proceedings Volume 9747, Terahertz, RF, Millimeter, and Submillimeter-Wave Technology and Applications IX, 13-18 February, 2016, San Francisco, California, edited by Laurence P. Sadwick and Tianxin Yang, 2016, p. 974707. © 2016 SPIE

As Published: http://dx.doi.org/10.1117/12.2209724

Publisher: Institute of Electrical and Electronics Engineers (IEEE)

Persistent URL: http://hdl.handle.net/1721.1/114643

Version: Final published version: final published article, as it appeared in a journal, conference proceedings, or other formally published context

Low-bias gate tunable terahertz plasmonic signatures in chemical vapour deposited graphene of varying grain size

Varun S. Kamboj, Philipp Braeuninger-Weimer, Piran R. Kidambi, David S. Jessop, Angadjit Singh, et al.

Varun S. Kamboj, Philipp Braeuninger-Weimer, Piran R. Kidambi, David S. Jessop, Angadjit Singh, Juraj Sibik, Yuan Ren, Stephan Hofmann, J. Axel Zeitler, Harvey E. Beere, David A. Ritchie, "Low-bias gate tunable terahertz plasmonic signatures in chemical vapour deposited graphene of varying grain size," Proc. SPIE 9747, Terahertz, RF, Millimeter, and Submillimeter-Wave Technology and Applications IX, 974707 (25 February 2016); doi: 10.1117/12.2209724

SPIE.

Event: SPIE OPTO, 2016, San Francisco, California, United States

Low-bias gate tunable terahertz plasmonic signatures in chemical vapour deposited graphene of varying grain size

Varun S. Kamboj*[a], Philipp Braeuninger-Weimer[b], Piran R. Kidambi[c], David S. Jessop[a], Angadjit Singh[a], Juraj Sibik[d],Yuan Ren[a], Stephan Hofmann[b], J. Axel Zeitler[d], Harvey E. Beere[a] and David A. Ritchie[a]

[a]Cavendish Laboratory, University of Cambridge, J. J. Thomson Avenue, Cambridge CB3 0HE, United Kingdom;
[b]Department of Engineering, University of Cambridge, 9 JJ Thomson Avenue, Cambridge, CB3 0FA, United Kingdom;
[c]Department of Mechanical Engineering, Massachusetts Institute of Technology, Cambridge, Massachusetts 02139, United States;
[d]Department of Chemical Engineering and Biotechnology, University of Cambridge, Pembroke Street, Cambridge CB2 3RA, United Kingdom

ABSTRACT

We report the characterization of centimeter sized graphene field-effect transistors with ionic gating which enables active frequency and amplitude modulation of terahertz (THz) radiation. Chemical vapour deposited graphene with different grain sizes were studied using THz time-domain spectroscopy. We demonstrate that the plasmonic resonances intrinsic to graphene can be tuned over a wide range of THz frequencies by engineering the grain size of the graphene. Further frequency tuning of the resonance, up to ~65 GHz, is achieved by electrostatic doping via ionic gating. These results present the first demonstration of tuning the intrinsic plasmonic resonances in graphene.
Keywords: Terahertz, graphene, ion-gel, surface plasmon resonance, frequency tunable, top gate.

1. INTRODUCTION

The Terahertz (THz) region of the electromagnetic spectrum has been the subject of extensive research during the past decade, due to the technological importance of this frequency range for various applications ranging from medical imaging and gas sensing to astronomy[1]. In particular plasmonics in graphene is of special interest, due to strong light-plasmon coupling in the graphene, which occurs at THz frequencies[2] (at room temperature) and can therefore be utilized in future THz components such as active optical modulators[3,4]. Graphene which is a two dimensional hexagonal arrangement of carbon atoms[5] with a myriad of properties[6] has been demonstrated to be an especially useful material for optoelectronic applications[7]. The unique optical properties of graphene, for instance the transmittance and absorption can be expressed solely in terms of the fine structure constant $\alpha = e^2/\hbar c = 1/137$, result from its unique band-structure where quasiparticles obey a linear dispersion relationship[8]. As a result the optical conductivity of undoped graphene is given by is given by $\sigma_{univ} = e^2/4\hbar$ and does not depend on any other parameter[8]. However doping graphene has a very strong effect on its optical properties[9]. Electrolytic gating graphene has been shown to achieve high doping concentration up to 10^{-13} cm^{-2} and has been used to achieve an amplitude modulation in the visible range[7]. Plasmonic resonances in graphene which occur in THz frequency range[2] can also be tuned by electrostatic doping via ionic gating and will be an essential feature of future photodetectors working at THz frequency range[10]. In a two- dimensional system the transverse magnetic plasmon mode in the long wavelength limit with $k \rightarrow 0$, the plasmonic frequency is given by $\omega_p(k) = \sqrt{(2Dk/\varepsilon}$, where $D = \pi n e^2/m^*$ is the Drude weight, ε is the dielectric constant of medium surrounding graphene and n is the charge carrier concentration. In graphene however the electrons behave as massless Dirac fermions and its Drude weight

*E-mail: vk302@cam.ac.uk , Phone: +44 1223 768142

Terahertz, RF, Millimeter, and Submillimeter-Wave Technology and Applications IX,
edited by Laurence P. Sadwick, Tianxin Yang, Proc. of SPIE Vol. 9747, 974707
 · doi: 10.1117/12.2209724

is given by $D_{dirac} = 4\sigma_{univ}E_f/\hbar$. This results in a modified relationship for plasmonic frequency in graphene given as $\omega_p(k) = \sqrt{(8kv_f\sigma_{univ}\sqrt{n})/\varepsilon}$, where v_f is the fermi velocity of carriers in graphene ~ 10^6 m/s, hence obeying a $\omega_p \propto n^{1/4}$ relationship[11]. Plasmons in graphene have been studied with various techniques such as angle-resolved photoemission spectroscopy (ARPES) and energy-loss spectroscopy (ELS) [12]. In an experiment with graphene in SiC substrate ELS showed the intrinsic surface plasmons in graphene strongly couple to the optical phonons of the SiC substrate[13]. Patterning graphene into micro-ribbon arrays, these surface plasmonic resonances can be engineered within the terahertz range as demonstrated by Long Ju *et. al.*[14]. Although plasmonic resonances in graphene meta-materials has been studied extensively[14-16], there are fewer reports about intrinsic plasmonic resonances resulting from scattering with domain boundaries in graphene. In this paper we used ionic top gating to induce charge carrier concentrations of up to 10^{-13} cm^{-2} probed plasmonic resonances in THz range by using THz time domain spectroscopy. We present a study of the intrinsic resonances which can be engineered by the growth conditions and can be further tuned using an ion gel top gate.

2. THEORETICAL BACKGROUND

Chemical Vapour Deposited (CVD) graphene is poly-crystalline in nature and the nucleation of graphene domains starts locally on the substrate of choice. Scattering of these plasma waves form the grain boundaries introduces resonances in the THz spectra, which could be studied with THz TDS. In a theoretical study by V. Ryzhii [17] a graphene field effect transistor has been shown to sustain plasma oscillations between highly conducting source-drain contacts. The plasma frequency scales linearly with the wave phase velocity, given by,

$$\omega(k) = \frac{kv_f}{\sqrt{1-\left(\frac{\alpha_g}{1+\alpha_g}\right)^2}} = k.s \tag{1}$$

where plasmon wave phase velocity *s* given by equation 2,

$$s = \frac{v_f}{\sqrt{1-\left(\frac{\alpha_g}{1+\alpha_g}\right)^2}} \tag{2}$$

If the phase velocity *s* exceeds the fermi velocity of Dirac quasiparticles in graphene then a plasma wave propagates at the interface between graphene and the ion gate. The phase velocity of such propagating plasma wave is a function of applied gate voltage via parameter α_g given as

$$\alpha_g = \sqrt{\frac{8e^3(V_{tg}-V_{CNP})W_d}{\varepsilon\hbar^2 v_f^2}} = \sqrt{\frac{8e^3(V_{tg}-V_{CNP})}{C_{tg}\varepsilon\hbar^2 v_f^2}} \tag{3}$$

In equation (3) V_{tg} is the applied gate voltage for an ion gel top gate, W_d is the width of the dielectric surrounding graphene, ε denotes the average dielectric constant of the material surrounding the graphene, while v_f ~ 1.1 × 10^6 m/s is the Fermi velocity of the electrons in graphene[18]. If this model is extended to account for the grains, then collective density oscillations of the electron liquid could form a standing wave after reflecting from the grain boundaries. Hence, we can substitute wave-vector *k* by, $(2n-1)\pi/d_{grain}$ where d_{grain} is the diameter of the grains in graphene. Substituting these value in equation 3 yields the following relationship for plasma frequency $\omega(k)$

$$\omega(k) = \frac{(2n-1)\pi}{d_{grain}\sqrt{1-\left(\frac{\alpha_g}{1+\alpha_g}\right)^2}} \tag{4}$$

For our measurements, C_{tg} is calculated to be ~ 2.2 μFcm^{-2} (using a Debye layer thickness = 2 nm, discussed in detail in section 4), while the top gate bias is typically V_{tg} = 0.5 V. Substituting these value in equation 4 we get plasma phase velocity as $s = 1.96 \times 10^6$ m/s. For graphene with a grain diameter of $d_{grain} = 20 \pm 2\ \mu m$, the theoretical value of plasmonic resonance is calculated to be $\omega_p(k) \sim 0.55$ THz. Indeed a plasmonic resonance at ~ 0.544 THz is experimentally observed for the same grain diameter, discussed in the measurements section.

3. GROWTH AND FABRICATION

The graphene was grown using the state of art chemical vapour deposition technique at 1050^{0}C ; by altering the relative pressure of H_2 and CH_4 gas in the CVD chamber, graphene samples with two different grain sizes (average diameter of 20 μm and 5 μm) were grown[19] and then transferred from Cu foil on to a Si/SiO_2 substrate.[20,21] The transfer process involves PMMA and results in p-doping of the graphene sheet, which is clearly observed during the transport measurements. Raman spectra confirmed the presence of monolayer graphene of good quality with the G peak at 1580 cm^{-1}.and a 2D peak at 2700 cm^{-1} Standard photo-lithography techniques were used to define a square area of (4 × 5) mm^2 of graphene and the remaining graphene was etched away using the oxygen plasma etching. This was followed by another photo-lithography step to define the source, drain and gate contacts and deposited with Ti/ Au by thermal evaporation.

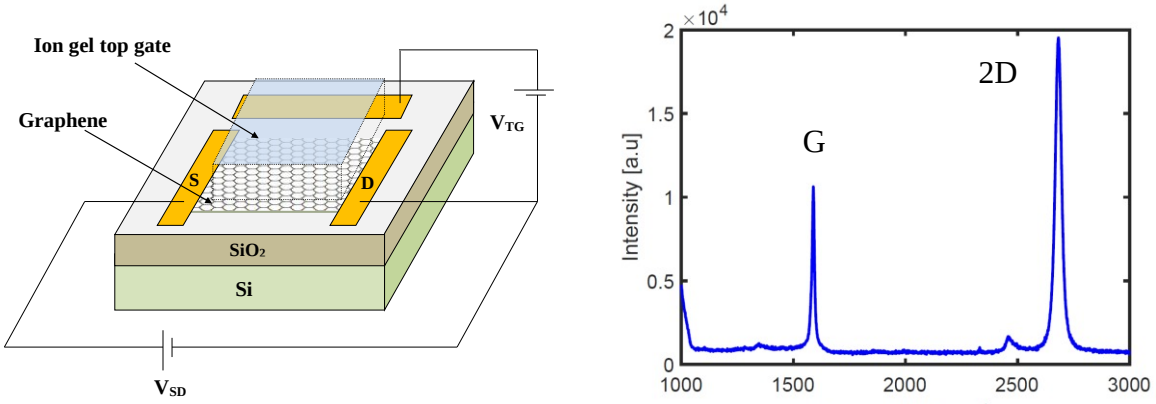

a) **b)**

Figure 1 a) Schematic of CVD graphene on Si/SiO_2 substrate. b) Raman spectroscopy of graphene with 2D and G peaks.

An ion gel composed of a mixture $LiClO_4$ in a polyethylene oxide matrix (in a ratio 0.14:1) was drop-cast on top of graphene to act as the top gate. The planar 2D geometry of the device structure allows for the gate contact to be isolated form the graphene sheet by 300 μm, hence reducing the leakage current. The sample with the ion gel on top was then annealed at 70^{0}C for 6 hours to remove any moisture form the sample. Using an ion gel top gate we could induce a charge carrier concentration $n \sim 10^{13}$ cm^{-2} by applying a small bias ~1.2 V. This is because of an increased capacitive interaction (~2 μFcm^{-2}) between the graphene sheet and the ion gate. In a back gate scenario, this capacitance is much smaller ~ 12 nFcm^{-2} due to thicker dielectric layer of SiO_2 (300 nm) between graphene and Si substrate. Therefore it requires ~100 V to induce a carrier concentration of $n \sim 10^{13}$ cm^{-2}, which can be induced using ion get top gate with ≤ 1V.

4. MEASUREMENTS

Electrical transport measurements were performed at room temperature and under a N_2 purged atmosphere, to improve the signal to noise ratio. Data acquisition was carried out using a HP spectrum Analyser in the configuration shown in the Fig.1 a). With an applied gate voltage V_{TG} as small as ~ 0.4 V we observed the charge neutrality point for the graphene

sample (with d_{grain} = 20 ± 2 μm) marking the neutralization of positive and negative charges in the graphene sheet [shown in Fig.2 a)]. A plot of the source-drain current I_{SD} as a function of V_{SD} at different top gate voltages V_{TG}, is shown in the Fig. 2 b).

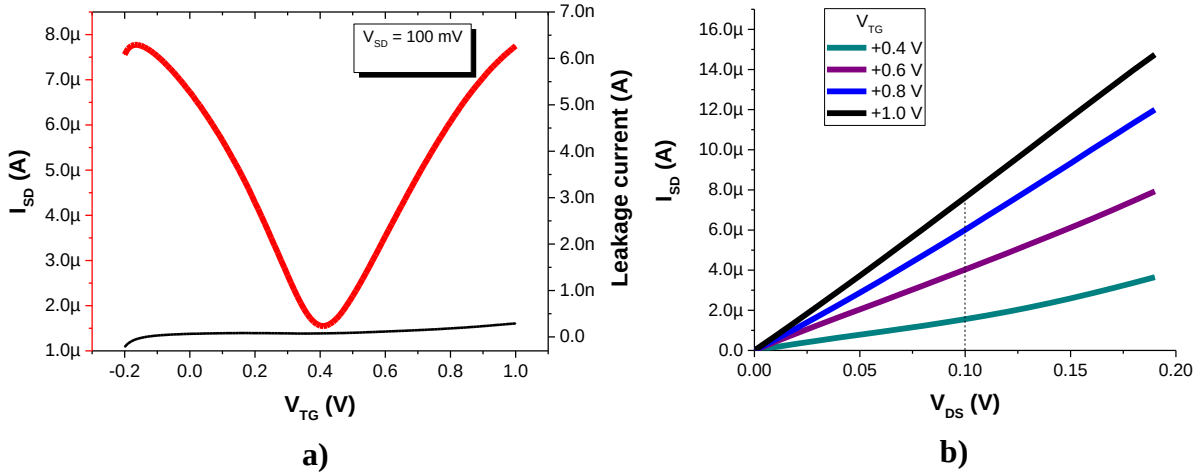

Figure 2 a) Plot showing V_{TG} vs. I_{SD} at a constant V_{SD} of 100 mV with the V_{CNP} at +0.4V b) Plot of I_{SD} vs. V_{DS}, the dotted line corresponds to the V_{DS} at which data in fig 2a) was measured.

The top gate voltage can be converted to an equivalent doping concentration, in the following way. Consider applying a top gate voltage of V_{TG} which creates a potential difference between the top gate and graphene, as well as shifts the fermi level E_F, such that,

$$V_{TG} = \frac{E_F}{e} + \phi \tag{5}$$

The term E_F / e is attributed to the chemical capacitance of graphene, while ϕ is related to the geometric capacitance between graphene and top gate[21]. The fermi energy in graphene varies with carrier concentration as $E_F(n) = \hbar v_f \sqrt{\pi n}$, where the fermi velocity[18], v_f = 1.1×10^6 m/s. The potential difference ϕ, generated between the graphene and top gate can be described by the following equation[22]

$$\phi = \frac{n e}{C_{TG}} \tag{6}$$

When a bias is applied to the gate contact (with respect to the drain electrode) the Li^+ ions accumulate near the negative electrode, while the ClO^-_4 ions collect near the positive electrode. This sets up an electric field inside the PEO matrix, which opposes the applied electric field from gate contact. Once an equilibrium is reached a space charge distribution is formed around the graphene, called the Debye layer. This Debye layer which is typically 2-5 nm thick acts as a parallel plate capacitor and we obtain a gate capacitance C_{TG} ~2.2 × 10-^{6} F cm^{-2}. From equation 5 we get the following relationship[22] between top gate voltage V_{TG} and the charge carrier concentration n

$$V_{TG} = 1.16 \times 10^{-7} \sqrt{n} + 0.723 \times 10^{-13} n \tag{7}$$

Equation 7 above can be used to estimate doping concentration as a function of top gate applied voltage. It can be observed that we obtain a minimum value of doping concentration n at a certain finite applied voltage. Fig. 3 a) shows a plot of doping concentration as function of top gate voltage. The voltage positive to V_{CNP} produce an electron doping, while

voltage negative to V_{CNP} creates a hole doping. A minimum charge carrier concentration and hence minimum conductivity is achieved when the fermi level is at the charge neutrality point (CNP). This is observed in the plot of sheet resistance vs. gate voltage in Fig. 3 b) where sheet resistance peaks at V_{TG} = 0.4V, suggesting that the fermi level is positioned at the CNP.

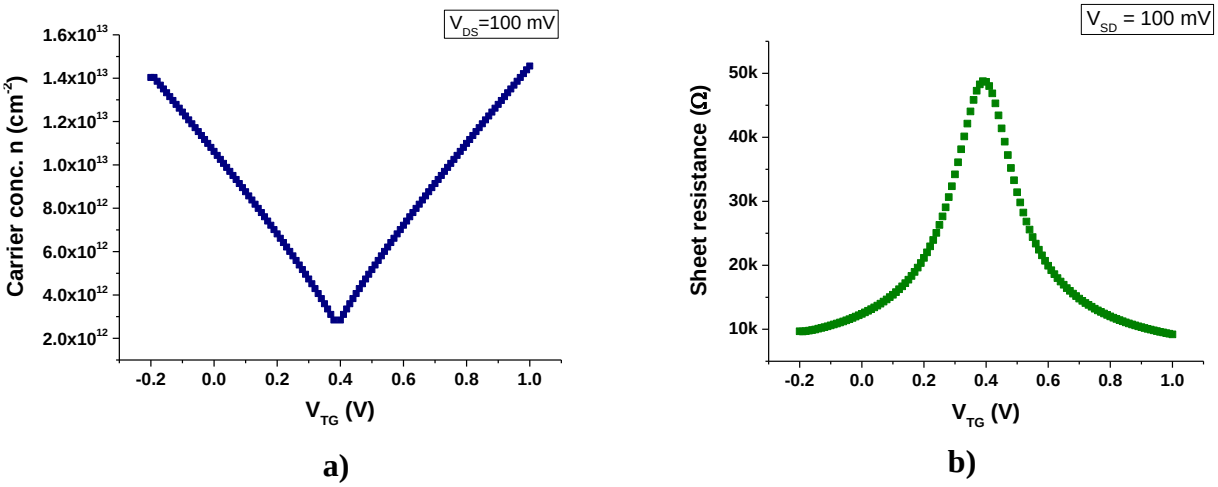

Figure 3 a) Plot showing Carrier concentration *n* vs. V_{TG} with the V_{CNP} at + 0.4V. *n* ~1.4× 10^{13} cm^{-2} is achieved at V_{TG} =1.0V b) Plot of Sheet resistance vs V_{TG}, with maximum resistance at the dirac point V_{CNP}

Broadband terahertz time domain spectroscopy (TDS) was carried out on gated graphene samples of two different grain sizes. Absorption spectra was deduced from the Fourier transform of the primary transmitted peak (through graphene) in the time domain and then normalized to the transmission at V_{CNP}, to probe the effect of gate voltage on the optical properties of graphene. From the absorption spectra plotted in the Fig. 4, we observe a prominent resonance feature at ~0.54 THz corresponding to the grain diameter of 20 μm and weaker resonant signatures at higher frequencies. The weaker features at ~1.0 THz and ~2.0 THz could be attribute to higher order dipoles of plasmonic oscillations within the grain boundaries.

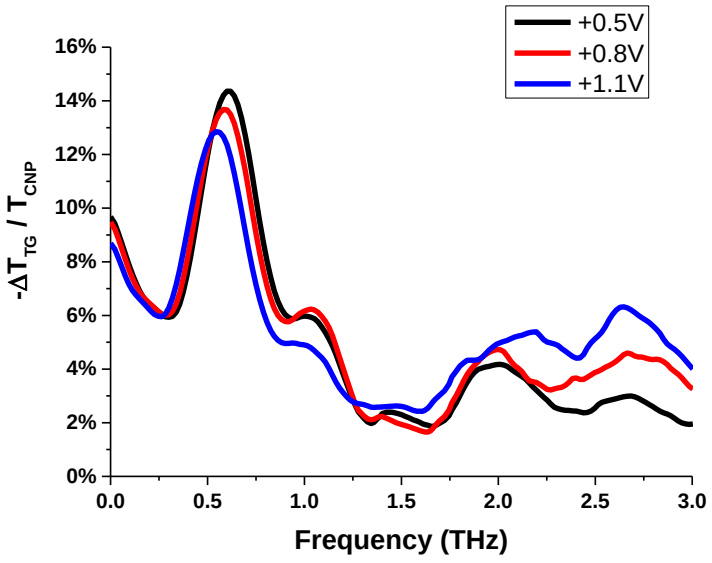

Figure 4. Absorption spectra showing of graphene sample with large domain size d_{grain} = 20 μm, at different gate bias. The prominent resonance features at ~0.54 THz is associated with the size of the graphene grains.

At a gate bias of 0.8V (+0.4V above the V_{CNP} = 0.4V) we observe that the resonant feature undergoes a blue-shift of 65 GHz, confirming the surface plasmonic origin of the observed features, in agreement with the theoretical value of ~0.55 THz calculated using equations (2-4) in section 2. Moreover with an applied gate voltage as low as 1.1 V we achieve an amplitude modulation of approximately 14 % due to the changing density of states available for the Drude like intraband absorption in graphene. The origin of such plasmonic features could be attributed to the polycrystalline nature of graphene and plasmon scattering at grain boundaries at high doping, induced by top gate.[23] In another sample having smaller grain sizes (Fig. 5) with the average diameter d = 5.0 μm, the plasmonic resonance is observed to be at ~2.7 THz, in close agreement with the theoretically calculated value of 2.693 THz, from equation2-4. The blue-shift in the THz frequency spectrum with reducing grain sizes is expected from Equation 4, having $\omega_p(k) \propto d_{grain}^{-1}$, where d_{grain}^{-1} is the average diameter of the graphene grain and is indeed observed clearly form Fig 4 and 5.

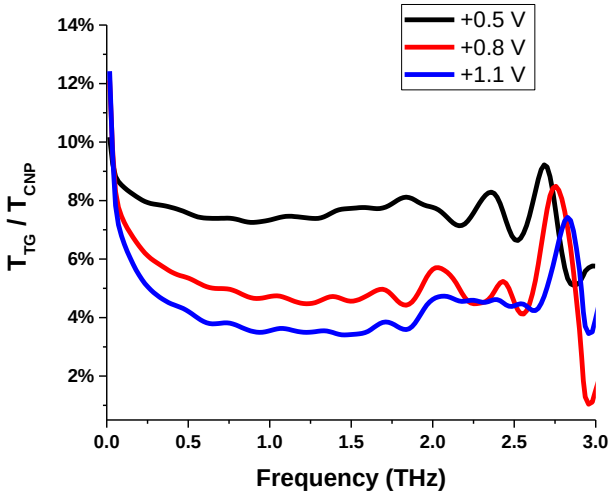

Figure 5. Transmittance of graphene sample with average grain diameter d_{grain} = 5.0 μm, at different gate bias. The resonance features observed at ~2.7 THz is related to the graphene grain size.

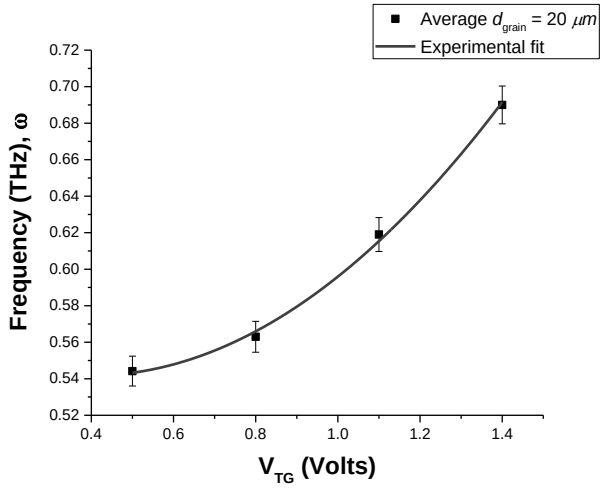

Figure 6. Plasmonic frequency ω_p as a function of applied top gate voltage V_{TG}. Data is fitted with a parabolic fit (black line)

With a grain size of 20 μm, as the top gate bias is increased beyond the V_{CNP} ~0.4 V, the charge carrier concentration increases form 3×10^{12} cm^{-2} to 1.4×10^{13} cm^{-2} at ~1.1 V. This causes the plasmonic frequency to vary with the applied gate voltage as $\omega_p(k) \propto \sqrt{V_{TG}}$.

The plasmonic resonances observed in graphene are also sensitive to the defects and the plasma oscillations gets damped during propagation. In order to improve S/N ratio and gain further understanding about the origin of these resonances, we could use a THz pump probe setup, where a pump source will illuminate the graphene and make the conductivity negative, due to a population inversion. In such a non-equilibrium state, the plasmonic oscillations would be amplified during propagation and much easier to detect with the THz probe beam.[24]

5. CONCLUSION

We have demonstrated the first realization of the gate tunability of intrinsic THz plasmonic signature in graphene. These plasmonic resonances can be engineered through CVD growth conditions, across the THz frequency range. The graphene with an average grain diameter d_{grain} = 20 μm revealed plasmonic resonances ~ 0.54 THz while grains with d = 5.5 μm showed a plasmonic response at ~2.7 THz. These plasmonic resonance could be further tuned by applying a top gate bias. For the 20 μm grain diameter, the plasmonic resonance at ~ 0.54 THz can be actively tuned and by modifying the charge carrier concentration n, using a top gate and we demonstrated a frequency tuning of up to 65 GHz. These results pave the way towards a better understanding of the origin the plasmonic resonances in graphene by relating them to the grain size in graphene. In conclusion this work not only provides fundamental insight into the plasmonic response of graphene grain and grain boundaries but also demonstrates a practical application of large area graphene, that is most sought after for future THz opto-electronic components.

6. ACKNOWLEDGMENTS

The authors of this manuscript acknowledge financial support from the Engineering and Physical Sciences Research Council (EPSRC), grant numbers EP/J017671/1 - Coherent Terahertz Systems (COTS) and EP/K016636/1- GRAPHTED.

REFERENCES

[1] Masayoshi Tonouchi, "Cutting-edge terahertz technology," *Nature Photonics* **1**, 97 - 105 (2007)
[2] E. H. Hwang and S. D. Sharma, "Dielectric function, screening, and plasmons in two-dimensional graphene," *Phys. Rev. B* **75**, 205418 (2007).
[3] S. Badhwar, R. Puddy, P.R. Kidambi, J. Sibik, A. Brewer, J.R. Freeman, H.E. Beere, S. Hofmann, J.A Zeitler, D. A. Ritchie, "Indirect Modulation of a Terahertz Quantum Cascade Laser Using Gate Tunable Graphene," *IEEE Photonics J*. **4**, 1776–1782 (2012).
[4] Q.Y. Wen, W. T. Q. Mao, Z. Chen, W. W. Liu, Q. H. Yang, M. Sanderson, Huai-Wu Zhang, "Graphene based All-Optical Spatial Terahertz Modulator," *Scientific Reports* **4**, 7409 (2014)
[5] K.S. Novoselov, A. K. Geim, S. V. Morozov, D. Jiang, M. I. Katsnelson, I. V. Grigorieva, S. V. Dubonos, A. A. Firsov, "Two-dimensional gas of massless Dirac fermions in graphene," *Nature* **438,** 197–200 (2005).
[6] A.K. Geim, K.S. Novoselov, "The rise of graphene," *Nature Mater.* **6,** 183–191 (2007).
[7] F. Bonaccorso, Z. Sun, T. Hasan, A.C. Ferrari, "Graphene photonics and optoelectronics," *Nature Photon.* **4,** 611–622 (2010).
[8] R.R. Nair, P. Blake, A.N. Grigorenko, K.S. Novoselov, T.J. Booth, T. Stauber, N.M.R. Peres, A.K. Geim, "Fine structure constant defines transparency of graphene," *Science* **320**, 1308–1308 (2008).
[9] Z. Q. Li, E. A. Henriksen, Z. Jiang, Z. Hao, M. C. Martin, P. Kim, H. L. Stormer, D. N. Basov, "Dirac charge dynamics in graphene by infrared spectroscopy," *Nature Phys.* **4,** 532–535 (2008).
[10] L. Vicarelli, M. S. Vitiello1, D. Coquillat, A. Lombardo, A. C. Ferrari, W. Knap, M. Polini, V. Pellegrini, A. Tredicucci, "Graphene field-effect transistors as room-temperature terahertz detectors," *Nature Mater*. **11**, 865–871 (2012).
[11] A. N. Grigorenko1, M. Polini, K. S. Novoselov, "Graphene plasmonics," *Nature Photonics* **6**, 749–758 (2012)

[12] T. Eberlein, U. Bangert, R. R. Nair, R. Jones, M. Gass, A. L. Bleloch, K. S. Novoselov, A. Geim, P. R. Briddon, "Plasmon spectroscopy of free-standing graphene films," *Phys. Rev. B* **77**, 233406 (2008).
[13] R.J. Koch, T. Seyller, J.A. Schaefer, "Strong phonon-plasmon coupled modes in the graphene/silicon carbide heterosystem," *Phys. Rev. B* **82**, 201413 (2010).
[14] Long Ju, B. Geng, J. Horng, C. Girit, M. Martin, Z. Hao, H. A. Bechtel, X.Liang, A. Zettl, Y. R. Shen, F. Wang, "Graphene plasmonics for tunable terahertz metamaterials," *Nature Nanotechnology* **6**, 630–634 (2011)
[15] R.Degl'Innocenti, D. S. Jessop, Y. D. Shah, J. Sibik, J. A. Zeitler, P. R. Kidambi, S. Hofmann, H. E. Beere, D A. Ritchie, "Low-Bias Terahertz Amplitude Modulator Based on Split-Ring Resonators and Graphene," *ACS Nano* 8(3), 2548–2554 (2014).
[16] S. Pleasants, "Graphene metamaterials," *Nature Photonics* **7**, 672 (2013)
[17] V. Ryzhii, "Terahertz Plasma Waves in Gated Graphene Heterostructures," *Japanese Journal of Applied Physics* **45**, 33–36 (2006).
[18] S. D. Sarma, S. Adam, E. Hwag, and E. Rossi, "Electronic transport in two-dimensional graphene," *Rev. Mod. Phys.* **83**, 407–460 (2011).
[19] P. R. Kidambi, B. C. BayeR, R. Blume, Z. J.Wang, C. Baehtz, R. S. Weatherup, M.G, Willinger, R. Schloegl,S. Hofmann, "Observing Graphene Grow: Catalyst–Graphene Interactions during Scalable Graphene Growth on Polycrystalline Copper," *Nano Lett.* **13** (10), 4769–4778 (2013).
[20] S. Hofmann, P. Braeuninger-Weimer, and R. S. Weatherup, "CVD-Enabled Graphene Manufacture and Technology," *J. Phys. Chem. Lett*., 2015, **6** (14), 2714–2721 (2015).
[21] P.R. Kidambi, C. Ducati, B. Dlubak, D. Gardiner, R. S. Weatherup, M.B. Martin, P. Seneor, H. Coles, S. Hofmann, "The Parameter Space of Graphene Chemical Vapor Deposition on Polycrystalline Cu," *J. Phys. Chem. C*, **116** (42), 22492–22501 (2012).
[22] A. Das, S. Pisana, B. Chakraborty, S. Piscanec, S. K. Saha, U. V. Waghmare, K. S. Novoselov, H. R.Krishnamurty, A. K. Geim, A. C. Ferrari, A. K. Sood, "Monitoring dopants by Raman scattering in an electrochemically top-gated graphene transistor," *Nature nanotechnology* **3**, 210 - 215 (2008)
[23] S. Badhwar, J. Sibik, P. R. Kidambi, H. E. Beere, J.A. Zeitler, S.Hofmann, D.A. Ritchie, "Intrinsic terahertz plasmon signatures in chemical vapour deposited graphene," *Appl. Phys. Lett.* **103**, 121110 (2013).
[24] M. Jablan, M. Soljacic, H. Buljan, "Plasmons in Graphene: Fundamental Properties and Potential Applications," *Proceedings of the IEEE* **7**, 1689-1704 (2013).